Cellular Automata Model of Cystogenesis and Tubulogenesis

Elhanan Borenstein[⋆]
[⋆]School of Computer Science
Tel Aviv University, Tel-Aviv 69978, Israel
borens@post.tau.ac.il

Erin Cline[†]
[†]Department of Molecular & Cellular Physiology
Stanford University, Stanford, CA 94305, USA
egcline@stanford.edu

Abstract

Cystogenesis and tubulogenesis are the processes by which cells form cysts and tubules. These processes are crucial for the formation of a variety of tissues (lungs, kidneys, intestines, etc). Using data from cell biology studies, we present a model of how such structures form from a collection of cells that do not initially have a lumen. Our model is an extension of the Cellular Potts Model (CPM), a commonly used framework for modelling and studying morphogenesis of multicellular constructs. In contradistinction to previous studies we integrate both local and global dynamics to formalize a realistic, yet simple, model of these processes. We further apply this model to validating the hypothesis that cysts and tubules are formed by the same generalized process and differ only in the initial geometry of the collection of cells.

1 Introduction

During development, individual cells interact with one another, proliferate, and rearrange themselves to produce tissues and organs. In cystogenesis (the making of a cyst) and tubulogenesis (the making of a tubule), cells enclose a hollow space, thus separating different compartments of the body. In many organs, this is how the function of the organ is established; the hollow space, termed a lumen, is utilized to transport some substance through the organ, wherein a particular physiological process occurs. For example, in the lung, bronchi (tubules) transport air into alveoli (cysts) where gas exchange with the blood takes place. In the kidney, nephrons carry blood through the organ so that it can be filtered and returned to the rest of the body free of wastes.

To study these fundamental processes of organogenesis, *in vitro* models of cystogenesis and tubulogenesis have been established in culture. Cells grown on two-dimensional supports have taught biologists about the structure of individual cells, but have failed to capture the details of the processes involved in forming multicellular tissues and organs. However, growing cells in a three-dimensional gel of extracellular matrix (ECM) proteins (e.g. collagen or Matrigel) allows cells to form cysts, and under certain conditions, tubules. One cell type that this method has been implemented in is the Madin-Darby Canine Kidney (MDCK) cell. When MDCK cells are grown in an ECM gel, they form hollow cysts. When treated with hepatocyte growth factor (HGF) these cysts develop branching tubules (Montesano et al., 1991; Pollack et al., 1998). The computational framework presented in this paper is based on and examines a model derived from observations made in this system.

Morphogenesis and organogenesis computational models have been the subject of numerous studies in recent years. One of the most promising frameworks for studying the formation of such multicellular structures is Cellular Automata (CA) models; in an analogous manner to organogenesis processes, cellular automata may produce complex, self-organizing constructs, while employing strictly short-range interactions (Wolfram, 2002). As such, they form an appealing and intuitive approach to modelling organogenesis. For an up-to-date introduction to work on cellular automaton approaches to modelling biological cells see Alber et al. (2002). One set of studies has employed the Lattice Gas Cellular Automata (LGCA) model, initially presented by Hardy et al. (1976) to model the molecular dynamics of a classical lattice gas. LGCA has been applied to model a wide range of multi-cellular behaviors including rippling, gliding and aggregation in myxobacteria (e.g. Börner et al., 2002; Alber et al., 2004) and cell alignment (e.g. Cook et al., 1997). However, LGCA models treat cells as

points on a lattice and thus cannot truthfully embody processes in which the shape of the cells changes over time and constitutes a crucial part of the process. In contrast, the Cellular Potts Model (CPM), described in detail in Section 3.1.1, is a flexible and powerful model that can exhibit complex cellular patterns. Graner and Glazier (1992) first presented the CPM for simulation of the differential adhesion hypothesis, demonstrating how it can produce patterns of biological cell sorting. Chaturvedi et al. (2003) and Izaguirre et al. (2004) presented COMPUCELL, a multi-modal software framework for simulation of morphogenesis, using as an example the formation of the skeletal pattern in the avian limb bud. CPM simulations were also used to simulate various stages of the slime mold *Dictyostelium discoideum* life cycle; Jiang et al. (1998), for example, applied a CPM based model to examine the contribution of differential adhesion and chemotaxis to the patterns that form in the mound stage. In this paper we extend these studies and present an enhanced CPM based framework of cystogenesis and tubulogenesis.

The remainder of this paper is organized as follows. We begin in Section 2 with a short description of the biological basis of our model. In particular we present our triphasic hypothesis. In Section 3 we introduce our computational model and describe in detail the local and global dynamics it incorporates. The simulation environment is briefly described in Section 4 and the results of a simulation run of the model are presented in Section 5. The paper concludes with a short description of future work.

2 Cystogenesis and Tubulogenesis in Biological Systems

Though cystogenesis and tubulogenesis create very different structures, there are some similarities. Both cysts and tubules are hollow structures enclosed by a layer of cells. In both cases, the cells enclosing the lumen are polarized: different proteins are localized to the membranes of the cells in contact with the lumen as opposed to the membranes in contact with other cells or the ECM. O'Brien et al. (2002) have proposed that not only do cysts and tubules share these characteristics but that the processes governing cystogenesis also govern tubulogenesis. Their model of cyst and tubule development, based on observations made in 3D cultures of MDCK cells, provides an elegant framework for understanding the common themes across the tremendous diversity of biological tubes seen during *in vivo* organogenesis (for reviews of cystogenesis and tubulogenesis see Hogan and Kolodziej, 2002; Lubarsky and Krasnow, 2003).

Cystogenesis is initiated by the formation of an aggregate of cells through proliferation and adhesion. Once such an aggregate has formed, O'Brien et al. hypothesize that cyst formation is driven by a *"three-surfaces pursuit"* (TSP). The first surface, in contact with the ECM, is the *basal* membrane. The second surface, which is in contact with other cells, is referred to as the *lateral* membrane. The third surface, in contact with the lumen, is the *apical* membrane. Upon initiation of the three-surfaces pursuit, the aggregate of cells creates these three surfaces through a combination of membrane separation, apoptosis, and directed protein delivery. In some systems, (e.g. mammary acini, Debnath et al., 2002), the apical membrane is defined when the cyst's inner cells die through *apoptosis* (programmed cell death) and form the lumen. In other systems, including MDCK cells, the apical surface is first brought about through the coalescence of vesicles (followed by apoptosis of any cells left in the lumen). Vesicles are small membrane-bound inclusions formed within a cell that can be filled with fluid and/or enzymes. When vesicles fuse together, they contribute to the separation of the membranes between cells and the formation of the lumen. Once the apical surface is defined, directed protein trafficking reinforces the identity of the other two surfaces (Figure 1a).

Upon treatment with HGF, tubules emanate from an MDCK cyst. O'Brien et al. suggest that this is achieved by a partial epithelial-mesenchymal transition (EMT) in cells receiving this "signal" from HGF, overriding the drive for three-surfaces. Cells undergoing a partial EMT grow out as chains of cells that exhibit reduced polarity and adhesiveness. According to O'Brien et al., when the HGF signal is attenuated, the cells of the chain are governed again by the same forces that initially led to the formation of the cyst. First, the cells proliferate and migrate to form a thick cord of cells. Then, triggered by resuming the TSP, a tubule will form: membranes are separated, cells left in the middle go through apoptosis, and directed protein trafficking defines the lateral and basal membranes of the cells (Figure 1b). Hence, this hypothesis posits that a cyst or a tubule can be formed by the same progression of signals. Only the initial geometries of the collection of cells (a radially symmetric

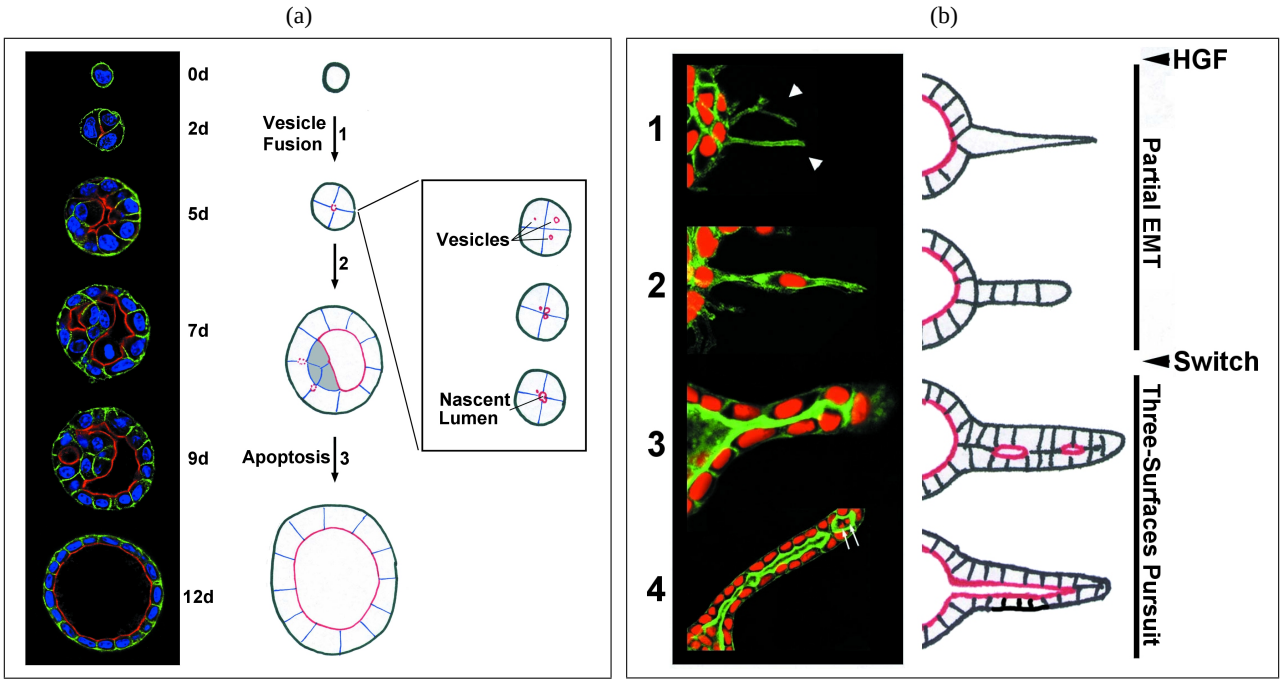

Figure 1: MDCK cyst development and HGF induced tubule formation. **(a)** Confocal images of MDCK cyst development in an ECM gel and a schematic of the process. A single cell at day 0 becomes a fully formed cyst at day 12. Vesicle fusion separates the membranes in the center of an aggregate of cells. As cyst development progresses, apoptosis clears the lumen of residual cells. **(b)** Treatment with HGF causes a cell of the cyst wall to undergo a partial EMT (1). After a chain of cells grows out (2), the TSP is triggered and a cord of cells develops (3). This cord then progresses to a tubule (4). Figures reproduced with permission from Nature Reviews Molecular Cell Biology, 3:531-537, 2002 (http://www.nature.com/reviews). Copyright 2002 Macmillan Magazines Ltd.

ball in the case of a cyst and an extended chain in the case of a tubule) dictate the final outcome. Based on this hypothesis, we present next the *cyclic triphasic model* of cytogenesis and tubulogenesis.

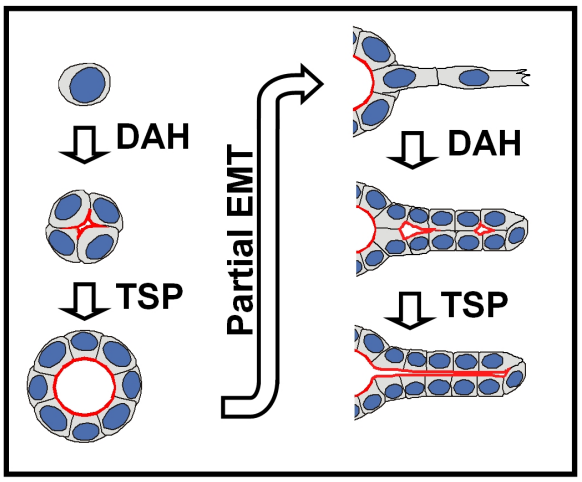

Figure 2: Schematic of cyst and tubule development. Proliferation and adhesion caused by DAH forces lead to an aggregate of cells. This aggregate becomes a cyst through TSP. The partial EMT causes a chain of cells to grow out. Resumption of DAH forces, followed by TSP, leads to tubule development. Illustration kindly provided by Lucy E. O'Brien and Keith Mostov, UCSF.

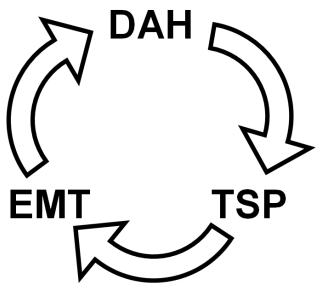

Figure 3: The Cyclic Triphasic Model of cystogenesis and tubulogenesis.

Starting from a single cell (Figure 2), the first stage of our model simulates proliferation and adhesion (referred to in the computational framework as DAH after the "Differential Adhesion Hypothesis" proposed by Steinberg, 1970). In this stage cells double their size and then divide in a random direction until a predetermined aggregate size is achieved. The cells adhere to each other preferentially over adhering to the ECM, thus forming a radially symmetric aggregate of cells. In the second stage, the TSP takes over. Cells in contact with the ECM become "apical cells" seeking an apical surface. They begin producing vesicles filled with a generalized "fluid" that will serve to enlarge and fill the lumen. At the same time, cells not in contact with the ECM go through apoptosis. In the third stage of the model, a "signal" representing a point source of HGF treatment is applied, causing one of the cyst cells to undergo a partial EMT. This cell divides in the direction of the signal and continues to grow and divide in this direction until the next signal is given. With the next signal, the cells in the chain again become subject to the DAH forces, forming a thick cord of cells through proliferation and adhesion. As with cyst development, this is followed by the TSP, in which vesicle formation and apoptosis create a lumen within the cord of cells, resulting in a tubule. The cycle could repeat again to form a branching structure; a new cell would receive the "signal" and progress through EMT, a new chain would be formed, and eventually this too would become a tubule. Thus, the cyclic triphasic model recapitulates *in silico* what is seen *in vitro* and, to some extent, what is seen *in vivo* during organogenesis (Figure 3).

3 The Model

Examining processes of organogenesis, one often discovers that the patterns, behavior and dynamics that can be detected vary dramatically when observing the system at different scales. Acknowledging this phenomenon, our model of tubulogenesis thus incorporates two distinct levels of dynamics: local dynamics, describing cells' morphogenesis, cell-cell interactions and other cell-level processes, and global dynamics, describing large-scale changes that affect the entire system. The local dynamics are based in part on the extended Cellular Potts model (Graner and Glazier, 1992), a commonly used framework for modelling multicellular processes. Our model incorporates additional extensions to support cell growth, division and apoptosis, as wells as vesicle formation, coalescence and fusion. The global dynamics are manifested as *signals* that can target all or a selected number of cells in the system. Signals affect local dynamics only indirectly by modifying the targeted cells' states, which in turn influence the local dynamics. This type of indirect interaction allows for a simple model, specified mostly in terms of local interaction rules, and provides a realistic framework for the processes that take place during organogenesis.

3.1 The Local Dynamics

3.1.1 The Cellular Potts Model

The local dynamics are based primarily on the two-dimensional extended Cellular Potts model (CPM), initially presented by Graner and Glazier (1992). The CPM is a sophisticated cellular-automata model for cell-level pattern modelling that can encapsulate cells' morphogenesis and cell-cell interactions. While being a biologically

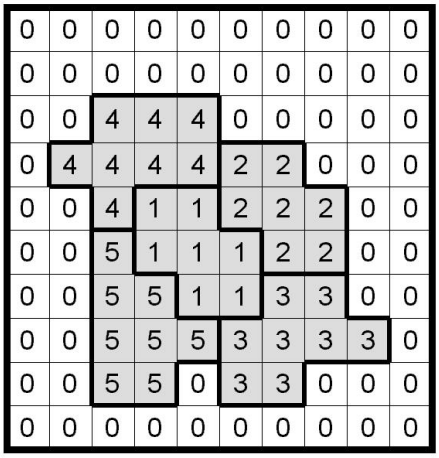

Figure 4: Schematic of a 2D CPM lattice. Different indices represent different cells. In our model, index 0 represents the ECM and index 1 represents fluid. The thick lines indicate cell boundaries (membranes). Drawing inspired by Alber et al. (2002).

realistic model, the main advantage of the CPM is its simplicity (Glazier and Graner, 1993): The dynamics require only local rules and local information while updating the status of the system. In the CPM, the system is described as a lattice, wherein each lattice site (i, j) is associated with an index $\sigma_{i,j}$. Sites with the same index are considered part of the same cell. Hence, in the CPM, in contradistinction to traditional cellular automata models such as LGCA, each cell is represented by a collection of lattice sites, providing a simple method of modelling cells of different sizes, shapes and membrane characteristics (Figure 4).

The dynamics of the system are governed by a simple Monte-Carlo process, aiming at minimizing some generalized utility function describing the "energy" of the entire system. The utility function can include various terms to describe the forces that apply to the system such as adhesion forces, cell surface minimization, chemotaxis, etc. In our model, the following Hamiltonian is used as the utility function:

$$\mathscr{H} = \sum_{\substack{(i,j),(i',j') \\ neighbors}} J(\tau(\sigma_{i,j}), \tau(\sigma_{i',j'}))(1 - \delta_{\sigma_{i,j},\sigma_{i',j'}}) + \lambda \sum_{\sigma} (S(\sigma) - S_{opt}(\sigma))^2 \quad .$$

The first term in the Hamiltonian accounts for adhesion forces between various cells and between cells and the Extracellular Matrix (ECM). $J(\tau, \tau')$ denotes the energy associated with the adhesion of a cell of type τ to a cell of type τ'. The second term accounts for the energy cost associated with a cell's size, $S(\sigma)$, differing from its optimal size, $S_{opt}(\sigma)$, where λ denotes an energy cost coefficient.

A Metropolis algorithm (Metropolis et al., 1953) is used to minimize the energy of the system: In each simulation time-step a lattice site (i, j) and a neighboring site (i', j') are selected at random. If the two sites have the same index nothing is changed and a new site is selected. Otherwise, a local change, wherein site (i, j) adopts the index of site (i', j'), is evaluated; the system's energy gain (or loss), $\Delta\mathscr{H}$, is calculated and the change is accepted with probability

$$P(\sigma_{i,j} \to \sigma_{i',j'}) = \begin{cases} 1 & \text{if } \Delta\mathscr{H} \leq 0 \\ \exp(-\Delta\mathscr{H}/T) & \text{if } \Delta\mathscr{H} > 0 \end{cases}$$

where $T > 0$ denotes the temperature of the system. One Monte Carlo step (MCS) is defined as as many trials (simulation time-steps) as the number of lattice sites. These minimization dynamics represent a competition between the forces that operate in the system and global geometric constraints (Alber et al., 2002).

3.1.2 Cell-States

Cells in our model can be in various *cell-states*[1] and may change their state due to local (e.g. cell division) or global (e.g. epithelial-mesenchymal transition) events. The cell-state determines several properties of the cell that may affect its behavior under the local dynamics process. In particular, for each cell-state, an *Optimal Size* parameter (S_{opt}) and *Adhesion Force* coefficients (J) are defined. These parameters are applied when calculating the Hamiltonian defined above and can thus dramatically affect the probability of accepting a certain local change. Hence, cells in different states exhibit markedly different behavior patterns, although they are governed by the same local dynamics processes. For example, changing the state of a cell from *Active* to *Growing*, wherein the *Optimal Size* parameter of a growing cell is defined as twice the optimal size of an *Active* cell, will cause the cell to inflate (and eventually divide). Similarly, changing the cell-state to an *Apoptosis* cell (which has an *Optimal Size* parameter of 0), will result in the cell tending to shrink and eventually disappearing.

Table 1 describes the various cell-states in our model and the parameter values assigned to each state. In addition to the parameters discussed above, *Growing* and *Growing-Chain* cells are also assigned with a *Preferred Division Direction*, used for the cell-division algorithms described in Section 3.1.3. It should be noted that the apoptosis process (wherein shrinking *Apoptosis* cells are being replaced by fluid) and the vesicle formation process yield an ever growing number of fluid sites, hence updating the *Optimal Size* parameter of the *Fluid* cell-state. It should also be noted that in our model *Mesenchymal* cells cannot be changed by the CPM dynamics and thus are not affected by adhesion forces.

Cell State/Type	Optimal Size	Adhesion Force Coefficient	Preferred Division Direction
ECM	No optimal size	-	-
Fluid	Changing	$J_{Fluid/ECM} = 100$	-
Active	C	$J_{Cell/ECM,Fluid} = 25$, $J_{Cell/Cell} = 15$	Not dividing
Growing	$2C$	$J_{Cell/ECM,Fluid} = 25$, $J_{Cell/Cell} = 15$	Along short axis
Apical	C	$J_{Cell/ECM,Fluid} = 25$, $J_{Cell/Cell} = 15$	Not dividing
Apoptosis	0	$J_{Cell/ECM,Fluid} = 25$, $J_{Cell/Cell} = 15$	Not dividing
Growing-Chain	$2C$	$J_{Cell/ECM,Fluid} = 25$, $J_{Cell/Cell} = 15$	Perpendicular to signal
Mesenchymal	C	No adhesion	Not dividing

Table 1: The different *Cell-States* in the model and the parameters assigned to each state. In the simulations described below the *Optimal Size* of a "normal" cell, C, is set to 30.

3.1.3 Extensions of the CPM

To capture some of the fine details involved in cystogenesis and tubulogenesis and to improve the resulting local dynamics, our model extends the CPM framework. The following extensions have been included:

E1: **Hexagonal Lattice:** In contrast to previous CPM studies, we use a hexagonal lattice which provides several advantages including a higher degree of symmetry and a better packing density (Fejes Tóth, 1960/1961).

E2: **Cell Division:** *Growing* and *Growing-Chain* cells (see Section 3.1.2) split when they reach their optimal size. Division is accomplished by assigning a new index to half the sites of the dividing cell. An analogous algorithm was also implemented in Chaturvedi et al. (2003).

E3: **Preferred Division Direction:** Dividing cells can have a preferred division direction, determining the orientation along which they will split. Cells can divide either along their shortest axis (as is the case in *Active* cells), or in a predefined direction (as in *Growing-Chain* cells which always split along the direction perpendicular to the direction of the EMT signal).

[1]The model also includes several cell "types" (namely, aside from cyst and tubule forming cells, ECM and Fluid), however, for simplicity, we handle these types as being additional cell-states.

E4: **Maximum Number of Divisions:** Each growing cell is initially assigned a parameter denoting the Maximum Number of Divisions (MND) it may go through. Whenever the cell divides, the two daughter cells are assigned an MND value equal to the MND of the mother cell minus 1. If after the cell division the two daughter cells have an MND value of 0, their state is modified to non-growing cells (in particular, *Growing* cells turn to *Active* cells and *Growing-Chain* cells turn to *Mesenchymal* cells).

E5: **Cell Break Prevention:** The standard CPM process may cause undesired cell breaks, whereby one cell splits into two unconnected parts. Our model includes a simple algorithm to identify such scenarios and prevent them.

E6: **Apoptosis Fluid Insertion:** To allow *Apoptosis* cells to shrink and eventually die out without collapsing the outer cyst or tubule, these cell are automatically replaced by fluid while shrinking. This modification is applied simply by assuming that the selected neighboring site of an *Apoptosis* site is always assigned a fluid index.

3.1.4 Vesicle Dynamics

In addition to the CPM energy minimization dynamics, the model employs an additional set of rules to simulate the formation of vesicles in apical cells and vesicle migration processes by which vesicles coalesce and fuse with the lumen. These dynamics are governed by the following two rules:

Rule 1: If the selected site is found to be: (i) associated with an apical cell, and (ii) an internal site (i.e. surrounded by sites with the same index), it turns into a vesicle site with probability $P_{vesicle}$ (0.015 in our simulation). Vesicle sites have the same index as fluid sites. Whenever a new vesicle is created, the optimal fluid size increases by 1 to allow such vesicles to coalesce within an apical cell and eventually fuse with the lumen's fluid. The *Optimal Size* parameter of the cell in which the vesicle forms remains unchanged, thus promoting regrowth of this cell. The total number of vesicles each apical cell can form is limited (20 vesicles per cell in our simulation) in order to prevent the overgrowth of the lumen.

Rule 2: If the selected site is a vesicle site, that is, it is: (i) associated with a fluid index, and (ii) surrounded by sites with indices different from fluid, it migrates towards the internal lumen. All six hexagonal directions are examined to determine the distance between the selected site and the ECM in each direction. The migration direction is then defined as the direction opposite to the one with the shortest distance to the ECM. Migration is performed by swapping the indices of the vesicle site with the neighboring site in the migration direction.

3.2 The Global Dynamics

The global dynamics encapsulate the various large-scale transitions that the system goes through (e.g. the epithelial-mesenchymal transition) and are implemented via a simple *Signaling* mechanism. Signals have three important characteristics: (i) they are a single time-point events, (ii) they cannot *directly* change the local dynamics, and (iii) being global events they can target many or all cells. In our model, signals affect the system by changing cell states. In particular, modelling the triphasic hypothesis, our model incorporates 3 distinct signals:

S1: **Proliferation and Adhesion (DAH)**: Changes all cells except for *Apical* cells to *Growing* cells. This allows cells to grow into an aggregate, but keeps an already formed cyst from changing. *Mesenchymal* cells turn into *Growing* cells with probability P_{m2g} (0.6 in our simulation) to prevent overgrowth of the cell cord.

S2: **Three Surface Pursuit (TSP)**: Changes all cells in contact with the ECM to *Apical* cells, and all other cells to *Apoptosis* cells. These cells also start forming vesicles.

S3: **Epithelial-Mesenchymal Transition (EMT)**: The signal is assumed to originate from the right side of the lattice and changes the cell closest to the source of the signal to a *Growing-chain* cell.

Triggering these signals in the appropriate order simulates the process of cystogenesis followed by tubulogenesis, and in particular can validate the triphasic hypothesis.

4 Simulation Software

The tubulogenesis model was implemented in C++ on MS-Windows operating system. The graphical interface employs native WinAPI. The Tubulogenesis Model Simulation Software (*TMSS*) is an interactive application, allowing the user to define various initial states of the system, trigger the available signals and turn the CPM dynamics on and off. The user interface of the application is illustrated in Figure 5. The application is available for download at: `http://www.cs.tau.ac.il/~borens/misc/tubu/CPMW_SIM.exe`.

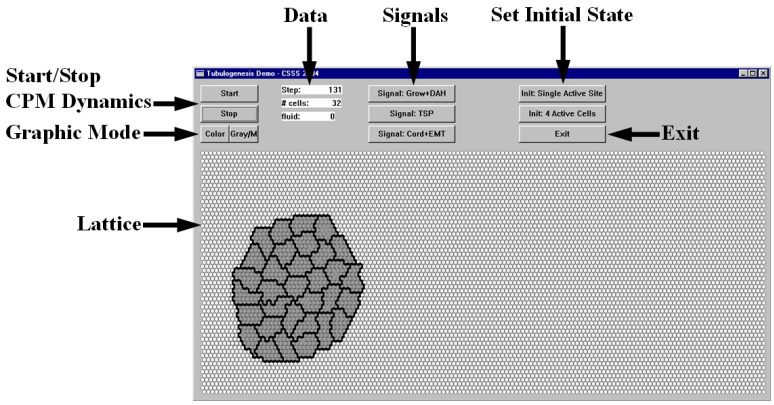

Figure 5: The Tubulogenesis Model Simulation Software user interface.

5 Results

This section describes the results of a sample simulation by our model. As demonstrated in Figure 6 and Figure 7, the cells' patterns that have emerged in our simulation are similar to those observed when MDCK cells are embedded in collagen, allowed to form cysts, and then stimulated with HGF. The simulation starts with one lattice site assigned with an index of an *Active* cell (all other site are assigned with the ECM index, 0). The first cell quickly grows to the size characterizing a normal cell (Figure 6a). Once the DAH signal is triggered, the cell starts growing and dividing, promptly constructing a ball of cells (Figure 6b). As *Growing* cells in our model are limited to 5 divisions, the ball reaches a size of 32 cells and stops growing (Figure 6c). After growth ceases, the DAH is still in effect and the ball of cells compacts as the cells minimize their contact with the ECM. The TSP signal then causes all internal cells to die out, forming a fluid-filled cyst (Figure 6d). The vesicles formed in the remaining *Apical* cells can also be seen in Figure 6d. As these vesicles coalesce and migrate away from the ECM the volume of the lumen is expanded. When the EMT signal is activated, the rightmost cell starts to grow and divide, eventually producing a chain of cells that grows towards the source of the signal (Figure 7a). Activating the DAH signal at this point re-enters the cycle that first produced the cyst, resulting in the cells of the chain proliferating and compacting to form a thicker cord of cells (Figure 7b). Following this cord formation with the TSP signal triggers the apoptosis of the cord's internal cells and the formation and fusion of vesicles in the external (now Apical) cells (Figure 7c), eventually generating a tubule (Figure 7d). Numerous simulation runs of the model were performed, yielding qualitatively similar results.

6 Future Work

The model described in this paper can be enhanced further to provide a more realistic model of tubulogenesis. In particular, there are two key modifications we wish to include. First, the chain growing process implemented

(a) Time step 18

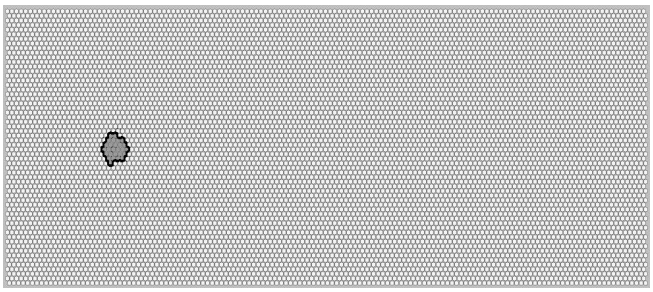

(b) Time step 44

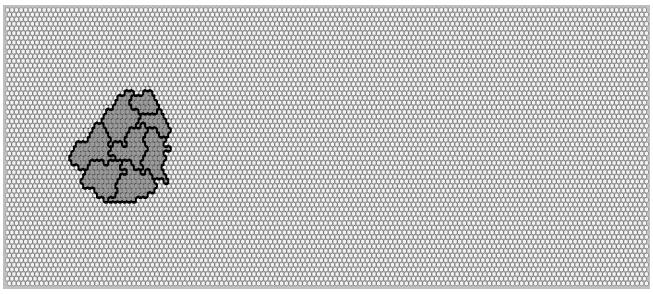

(c) Time step 131

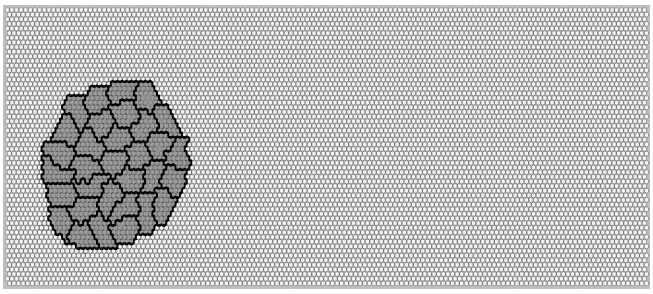

(d) Time step 175

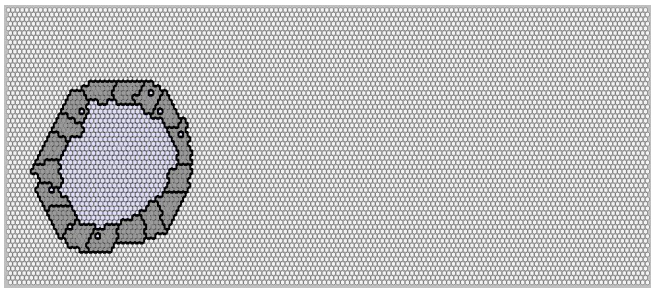

Figure 6: Cystogenesis. Time is measured in Monte Carlo steps (MCS). White sites indicate ECM and light gray-blue sites indicate fluid. The dark gray sites represent sites that are associated with cells. Cell boundaries are illustrated as thick black lines.

now produces thin cells which adhere to each other along their elongated surfaces. This phenomenon, induced by the *Mesenchymal* cells' properties in our model, does not match observed data. We intend to add *Chemotaxis* as an additional force in the CPM dynamics to govern the growth of the chain and hopefully produce patterns similar to the ones observed in experiments. Second, the signaling mechanism incorporated in our model utilizes distinct, non-overlapping phases. Cells growing in an ECM gel do not exhibit such distinct phases. Instead, the transition of cells from one state to another is more gradual. For example, vesicles start to form while the cells are still growing, and then continue to form and coalesce during the TSP phase, eventually creating a single, central lumen. We thus intend to enhance the global dynamics mechanism to allow for such overlapping phases.

(a) Time step 663

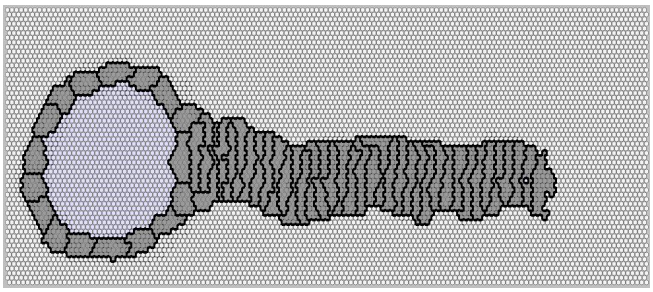

(b) Time step 720

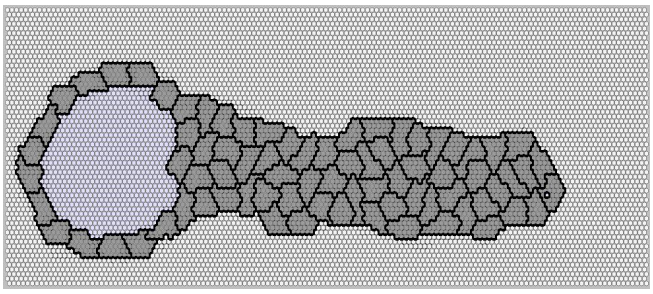

(c) Time step 726

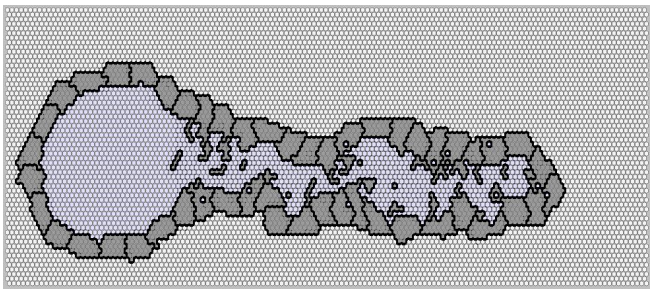

(d) Time step 833

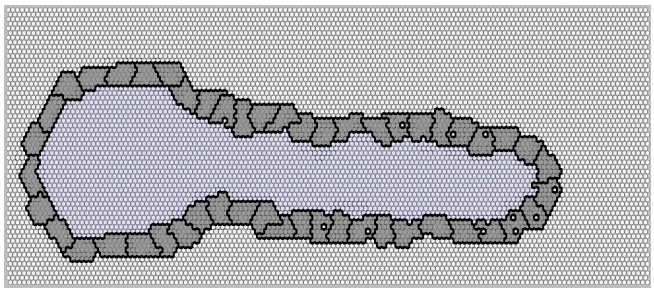

Figure 7: Tubulogenesis. Site color-code is the same as that used in Figure 6.

One possible approach is to include various local events that can trigger the onset of the global signals. Further extensions of the model are currently being developed.

7 Acknowledgements

This work originated and was partially carried out during the Santa Fe Institute - Complex Systems Summer School, 2004. The authors are grateful to the summer school faculty for their support and inspiration. The authors also wish to thank Keith Mostov, Lucy O'Brien, Anirban Datta and other members of the Mostov Lab at UCSF for their assistance and valuable feedback.

References

M.S. Alber, A. Kiskowski, and Y. Jiang. Lattice gas cellular automata model for rippling and aggregation in myxobacteria. *Physica D*, 191:343–358, 2004.

M.S. Alber, M.A. Kiskowski, J.A. Glazier, and Y. Jiang. On cellular automaton approaches to modeling biological cells. In D.N. Arnold and F. Santosa, editors, *Mathematical Systems Theory in Biology, Communication, and Finance*, pages 1–40, New York, 2002. Springer-Verlag.

U. Börner, A. Deutsch, Reichenbach. H., and M. Bar. Rippling patterns in aggregates of myxobacteria arise from cell-cell collisions. *Phys. Rev. Lett.*, 89(7):4473–4478, 2002.

R. Chaturvedi, J.A. Izaguirre, C. Huang, T. Cickovski, P. Virtue, G. Thomas, G. Forgacs, M. Alber, G. Hentschel, S.A. Newman, and J.A. Glazier. Multi-model simulations of chicken limb morphogenesis. In P.M.A. Sloot, D. Abramson, A.V. Bogdanov, J.J. Dongarra, A.Y. Zomaya, and Y.E. Gorbachev, editors, *Computational Science ICCS 2003: Proceedings, Part III*, pages 39–49, New York, 2003. Springer-Verlag.

J. Cook, A. Deutsch, and A. Mogilner. Models for spatio-angular self-organization in cell biology. In W. Alt, A. Deutsch, and G. Dunn, editors, *Dynamics of cell and tissue motion*, pages 173–182, 1997.

J. Debnath, K.R. Mills, N.L. Collins, M.J. Reginato, S.K. Muthuswamy, and J.S. Brugge. The role of apoptosis in creating and maintaining luminal space within normal and oncogene-expressing mammary acini. *Cell*, 111:29–40, 2002.

L. Fejes Tóth. On the stability of a circle packing. *Ann. Univ. Sci. Budapestinensis, Sect. Math.*, 3-4:63–66, 1960/1961.

J.A. Glazier and F. Graner. Simulation of the differential adhesion driven rearrangement of biological cells. *Physical Review E*, 47:2128–2154, 1993.

F. Graner and J.A. Glazier. Simulation of biological cell sorting using a two-dimensional extended potts model. *Physical Review Letters*, 69:2013–2016, 1992.

J. Hardy, Y. Pomeau, and O. de Pazzis. Molecular dynamics of a classical lattice gas: Transport properties and time correlation functions. *Phys. Rev. A*, 13:1949–1961, 1976.

B.L. Hogan and P.A. Kolodziej. Organogenesis: molecular mechanisms of tubulogenesis. *Nat. Rev. Genet.*, 3: 513–523, 2002.

J.A. Izaguirre, R. Chaturvedi, C. Huang, T. Cickovski, J. Coffland, G. Thomas, G. Forgacs, M. Alber, S.A. Newman, and J.A. Glazier. Compucell, a multi-model framework for simulation of morphogenesis. *Bioinformatics*, 20:1129–1137, 2004.

Y. Jiang, H. Levine, and J.A. Glazier. Possible cooperation of differential adhesion and chemotaxis in mound formation of *dictyostelium. Biophysical Journal*, 75:2615–2625, 1998.

B. Lubarsky and M.A. Krasnow. Tube morphogenesis: making and shaping biological tubes. *Cell*, 112:19–28, 2003.

N. Metropolis, A. Rosenbluth, M. Rosenbluth, A. Teller, and E. Teller. Combinatorial minimization. *J. Chem. Phys.*, 21:1087–1092, 1953.

R. Montesano, G. Schaller, and L. Orci. Induction of epithelial tubular morphogenesis in vitro by fibroblast-derived soluble factors. *Cell*, 66:697–711, 1991.

L.E. O'Brien, M.M. Zegers, and K.E. Mostov. Opinion: Building epithelial architecture: insights from three-dimensional culture models. *Nat. Rev. Mol. Cell. Biol.*, 3:531–537, 2002.

A.L. Pollack, R.B. Runyan, and K.E. Mostov. Morphogenetic mechanisms of epithelial tubulogenesis: Mdck cell polarity is transiently rearranged without loss of cell-cell contact during scatter factor/hepatocyte growth factor-induced tubulogenesis. *Dev. Biol.*, 204:64–79, 1998.

M.S. Steinberg. Does differential adhesion govern self-assembly processes in histogenesis? equilibrium configurations and the emergence of a hierarchy among populations of embryonic cells. *J. Exp. Zool.*, 173:395–433, 1970.

S. Wolfram. *A new kind of science*. Wolfram Media Inc., 2002.